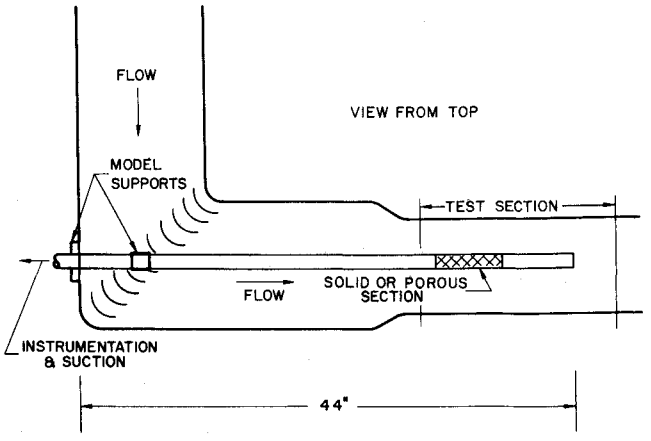

Fig. 3 Model installation.

Experimental study

Model design and installation: To demonstrate the technique, a cylindrical base pressure model (Fig. 2) was designed, fabricated, and tested in the Boeing Model Transonic Wind Tunnel and Boeing Model Supersonic Wind Tunnel. Pressure taps were installed on the cylinder surface as well as on the base. A porous section made of Rigimesh with 10% porosity was installed for boundary-layer control (Fig. 3). No flow perturbations were generated by the supporting structure affecting the base flow.

Results

Boundary-layer thickness

The boundary-layer thickness was measured by use of a Pitot probe. It was found that the boundary layer is essentially completely bled and its growth was reinitiated at the end of the porous section. The shape of the boundary-layer profile also indicated that the flow was turbulent.

Base pressure without suction

The base pressure as a function of Mach number is shown in Fig. 4. The results of free flight data as obtained by Hart[1] are also shown in the figure for comparison. There is reasonable agreement between the present wind-tunnel test and the free flight results.

Strut effects

For the model and Mach number range under consideration, it was found that the effects of the strut are to increase the base pressure slightly.

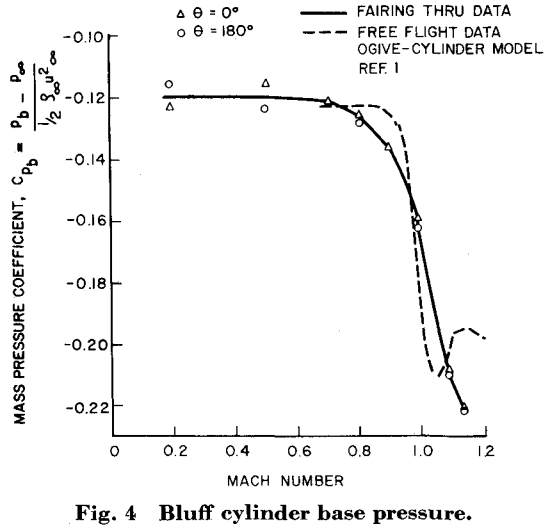

Fig. 4 Bluff cylinder base pressure.

Boundary-layer effects

The effect of boundary-layer thickness on the base pressure was found by measuring the base pressure with and without suction. In general, the base pressure is slightly higher with thicker boundary layer (without suction) than that with thinner boundary layer (with suction).

The base pressure as a function of momentum thickness at various Mach numbers was also determined. In general, the base pressure increases as the boundary-layer thickness increases. Also, there appears to be a critical boundary-layer thickness. Below this critical value, the base pressure is a strong function of the boundary-layer thickness. Above this critical value, the dependence of base pressure on the boundary-layer thickness is relatively insignificant.

Conclusions

The dimensionless base pressure in subsonic and supersonic flow is governed by two parameters: the Mach number and the dimensionless boundary layer thickness. This suggests the use of a long cylindrical body and boundary layer suction in place of the conventional mountings for base pressure models. The cylindrical body is extended and supported far upstream so that there is no strut to interfere with the flow. The boundary-layer thickness is controlled by use of suction ahead of the base pressure model. This scheme has been successfully demonstrated for the case of subsonic and transonic flows.

Reference

[1] Hart, R. G., "Effects of Stabilizing Fins and a Rear-Support Sting on the Base Pressures of a Body of Revolution in Free Flight at Mach Numbers from 0.7 to 1.3," RM L52E06, Sept. 1952, NACA.

Film-Cooling on the Anode of a Plasma Generator

L. Berkley Davis Jr.* and Clifford J. Cremers†
University of Kentucky, Lexington, Ky.

An investigation of the operating characteristics of an arc plasma generator whose anode is protected both by film- and water-cooling has been undertaken. Such a device allows the use of a refractory material for the anode without substantial ablation but does not yield the high conversion efficiency of electrical to thermal energy found previously with a purely film-cooling anode.[1] The apparatus[2] consists of a cathode section, a stack of four constrictor segments, and an anode assembly.

Argon is injected tangentially at the base of the constrictor stack, flows through the constrictor channel in contact with the electric arc, mixes with the film gas (also argon) at the upstream edge of the anode, and flows from the anode into a calorimeter. The film flow is injected radially and is turned so that it flows parallel to the anode surface by a slot formed by a boron-nitride nozzle and the graphite anode. The flow channel in the constrictor stack is of 9.54-

Received March 29, 1971; revision received May 24, 1971. Research supported in part by the National Science Foundation under Grant GK 1243.

Index categories: Electric and Advanced Space Propulsion; Plasma Dynamics and MHD.

* Graduate Student in Mechanical Engineering. Student Member AIAA.

† Professor of Mechanical Engineering. Member AIAA.

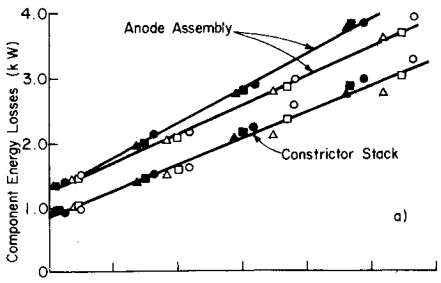

Fig. 1a Constrictor stack and anode assembly losses vs power input.

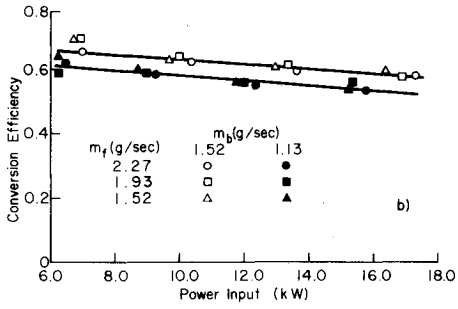

Fig. 1b Energy conversion efficiencies vs power input for current levels of 126, 171, 214, and 258 amp.

mm diam and of length 27.4 mm while the corresponding dimensions for the anode are 12.7 mm and 11.1 mm. Cremers et al.[1] discuss the choice of materials and the anode configuration.

The energy losses to the constrictor stack and the anode assembly are shown in Fig. 1a for film flow rates ($\dot{m}_f$) of 2.27, 1.93, and 1.52 g/sec, base flow rates ($\dot{m}_b$) of 1.52 and 1.13 g/sec, and for current levels of 126, 171, 214, and 258 amp. The obvious grouping of the data points arises from variation in the arc voltage drop when the arc current is maintained constant but the argon flow rates are changed. The losses to the constrictor stack show little dependence on the film and base flow rates except as those flow rates affect the electric field, and thereby the arc voltage drop, in the constrictor channel. Such an effect of the base flow is expected, while that of the film flow shows that the film does exert a squeezing effect on the arc in the anode throat, can cause a slight increase in density upstream, and thus affects the electric field and the heat transfer coefficient. This is not a large effect; in fact, a 15% increase in $\dot{m}_f$ with constant $\dot{m}_b$ will cause about a 3% change in the over-all arc voltage drop.

The energy transferred to the anode by the electrons, which constitute almost all of the arc current and which condense on the anode surface, is the dominant energy input to the anode assembly (in contrast to the constrictor stack losses that depend on the flow and electric fields as well as the arc current, i.e., the rate at which the energy is dissipated, within the constrictor channel). An increase in the base flow rate causes an increase in the arc voltage drop; thus, for a given power input, the arc current and the anode assembly losses are smaller. This effect accounts for the dependence of the anode assembly losses on the base flow rate.

A decrease in the film flow rate lessens the protection provided by the film and the anode surface temperature will increase. This leads to the more diffuse arc attachment explained in Ref. 1. Visual observations of the incandescent portion of the anode surface confirm that, as either the film flow is decreased while maintaining constant current and base flow or as the current is increased at constant argon flow rates, the arc attachment area increased. The data also show that the energy loss at the anode decreased for smaller $\dot{m}_f$ and constant current and $\dot{m}_b$. A smaller anode fall voltage accounts for this.

The visual observations also showed that the tangential injection of the base flow did not drive the arc attachment point circumferentially over the anode surface in the ranges of flow rates considered. Increasing the base flow rate to the maximum obtainable with the equipment available (2.27 g/sec) and decreasing the film flow rate to the point where rapid ablation of the anode occurred (1.0 g/sec) did not cause the arc attachment to move. Radial injection of the base flow and tangential injection of the film should alleviate this difficulty.

The energy conversion efficiency is defined as the energy output to a calorimeter divided by power input and is shown versus power input in Fig. 1b. A clear dependence on the base flow rate exists while the film flow rate has only a small effect. The efficiencies are comparable with, or at best only slightly higher than, those of similar generators with purely water-cooled anodes. Variation of the cooling water flow to the anode has only small effects in the range considered (0.064–0.079 kg/sec).

References

[1] Cremers, C. J., Shiver, W. D., and Birkebak, R. C., "Film-Cooling of a Plasma Generator Anode," *AIAA Journal*, Vol. 6, No. 9, Sept. 1968, pp. 1774–1776.

[2] Davis, L. B., "A Study of Film-Cooling on the Anode of an Arc Plasma Generator," M.S. thesis, May 1970, Univ. of Kentucky, Lexington, Ky.

Roughness Effects on Heat Transfer in the Supersonic Region of a Conical Nozzle

MEYER RESHOTKO*
NASA Lewis Research Center, Cleveland, Ohio

As part of the study on the effects of roughness in conical nozzles heat-transfer results were obtained in the supersonic region up to Mach 4.4. This paper will concentrate on the region between Mach 1.7 and 4.4 where the acceleration drops off from the high values in the vicinity of the throat to the low values near the nozzle exit. This is an area of particular interest to those who use rough surfaces to simulate the effects of ablation that take place upon re-entry. A material such as graphite after undergoing ablation will have a surface texture similar to those discussed in this paper.

A number of experiments have been recently conducted (Ref. 1-6) on the effects of flow acceleration with and without surface roughness on heat transfer. In these cases the favorable pressure gradient was obtained by passing the working fluid through a converging-diverging nozzle. Flow acceleration represented by velocity and pressure gradient are shown in Fig. 1 as a function of axial distance from the throat. Main interest was directed at the region of highly accelerated flow which is upstream of and in the vicinity of the throat. It was in this region that there was an appreciable difference between the experimental heat-transfer results and the existing correlations. The results are given in detail in Refs. 4–6 and summarily in Fig. 2 for the representative case of $M = 0.48$. It can be seen (Fig. 2) that for a smooth wall there are two distinct regimes of heat-transfer rate that

Received April 8, 1971.

* Aerospace Research Engineer. Associate Member AIAA.